Geophysical Research Letters

RESEARCH LETTER
10.1029/2018GL078125

Key Points:
- The iron spin transition does not alter the long-term stability of large primordial reservoirs in the lower mantle
- The iron spin transition slightly enhances the convection vigor and produce more entrainments to the upper mantle by plumes
- The iron spin transition helps to build slightly sharper sides of large primordial reservoirs

Supporting Information:
- Supporting Information S1

Correspondence to:
Y. Li and K. Vilella,
yli@mail.iggcas.ac.cn;
vilella@earth.sinica.edu.tw

Citation:
Li, Y., Vilella, K., Deschamps, F., Zhao, L., & Tackley, P. J. (2018). Effects of iron spin transition on the structure and stability of large primordial reservoirs in Earth's lower mantle. *Geophysical Research Letters*, *45*. https://doi.org/10.1029/2018GL078125

Received 30 MAR 2018
Accepted 21 MAY 2018
Accepted article online 29 MAY 2018

Effects of Iron Spin Transition on the Structure and Stability of Large Primordial Reservoirs in Earth's Lower Mantle

Yang Li[1,2,3], Kenny Vilella[4], Frédéric Deschamps[4], Liang Zhao[1,2,3], and Paul J. Tackley[5]

[1]State Key Laboratory of Lithospheric Evolution, Institute of Geology and Geophysics, Chinese Academy of Sciences, Beijing, China, [2]Institutions of Earth Science, Chinese Academy of Sciences, Beijing, China, [3]Laboratory for Marine Mineral Resources, Qingdao National Laboratory for Marine Science and Technology, Qingdao, China, [4]Institute of Earth Sciences, Academia Sinica, Taipei, Taiwan, [5]Institute of Geophysics, Department of Earth Sciences, ETH Zurich, Zurich, Switzerland

Abstract Experimental and theoretical studies have shown that the iron spin transition alters the properties of lower mantle minerals. This may have important implications for mantle dynamics. In particular, the vigor of convection is enhanced, which in turn may impact the stability of large primordial reservoirs at the base of the lower mantle. Here we performed numerical experiments of thermochemical convection in 2-D annulus geometry including the change of density induced by iron spin transition. Our results show that this density change only slightly affects mantle dynamics by increasing the convection vigor. This, in turn, slightly increases the entrainment of primordial dense materials by plumes and leads to smaller reservoirs with sharper edges. However, this effect is small compared to those of the intrinsic density contrast between the dense primordial and regular mantle materials, which is the dominant parameter controlling the long-term stability of the large primordial reservoirs.

Plain Language Summary Experimental and theoretical studies suggested that transition in the spin state of iron occur in the lower mantle minerals at lower mantle pressure and that it may have important implications for mantle dynamics. In this study, we performed 2-D numerical experiments of thermochemical mantle convection implemented with a recent mineral data set as density input. We find that the dynamic effects of the iron spin transition on the lower mantle's thermochemical structures are small. The main parameter controlling the long-term stability of large primordial reservoirs in the lower mantle remains the chemical density contrasts between the primordial material and ambient mantle material that controls.

1. Introduction

Seismological studies suggest the presence in the deep Earth's mantle of two antipodal large low shear velocity provinces (LLSVPs) beneath Africa and the Pacific (e.g., He & Wen, 2012; Masters et al., 2000; Ni et al., 2002; Wang & Wen, 2007). These LLSVPs cover up to 30% of the core-mantle boundary (CMB) region and are characterized by a reduction of shear velocity (see review by Garnero et al., 2016, for more details). Although the nature of LLSVPs, purely thermal or chemically distinct structures, is still under debate (e.g., Garnero et al., 2016), several evidences including deep mantle density variations inferred from seismic normal modes data (Ishii & Tromp, 1999; Mosca et al., 2012; Trampert et al., 2004), and solid tides (Lau et al., 2017) indicate that LLSVPs are denser than average mantle and may thus have a distinct composition. By contrast, Kuo and Romanowicz (2002) pointed out that normal modes may not be able to resolve the lower mantle density structure, and a recent study based on Stoneley modes, which are mostly sensitive to the bottom of the mantle and the top of the core, concluded that LLSVPs are less dense than surrounding mantle (Koelemeijer et al., 2017). Assuming that LLSVPs are chemically distinct reservoirs raises important questions concerning their origin. To solve this issue, it has been suggested that they have formed early in Earth's history (Torsvik et al., 2014), i.e., resulting from mantle partial differentiation (e.g., Labrosse et al., 2007; Solomatov & Stevenson, 1993), in which case they may consist of reservoirs of primitive undegassed materials. This hypothesis is further supported by geochemical observations, in particular the high $^{142}Nd/^{144}Nd$ ratios (Boyet & Carlson, 2006; Hofmann, 1997) and the dispersion of helium isotopic ratio, $^{3}He/^{4}He$, in oceanic island basalts (Farley et al., 1992; Lupton & Craig, 1975). Assuming that LLSVPs have formed early in Earth's history implies that they remained mostly

stable throughout the whole Earth's evolution, i.e., their properties prevented significant entrainment by mantle convection although they may have experienced migration or change in shape.

Importantly, the dynamics of the mantle, and therefore the evolution of the LLSVPs, is strongly influenced by the physical properties of the minerals of the mantle, including their density. The main parameters affecting density are temperature and composition, but other effects, especially an iron spin transition, may also alter its value. A theoretical study by Fyfe (1960) predicted that the electronic structure of Fe^{2+} in the octahedral coordination can change at high pressure, and that this transition may occur under the pressure-temperature conditions of the Earth's lower mantle (e.g., Cohen et al., 1997). Experimental studies confirmed this phenomenon, referred to as the iron spin transition, and observed it in both ferropericlase (Fp; Badro et al., 2003) and bridgmanite (Bm; Badro et al., 2004; Jackson et al., 2005) the two major minerals of the lower mantle. In Fp, Fe^{2+} is located in octahedral sites such that its 3*d* orbital is split in two energy levels. At ambient condition, the high spin state is stable with electrons present in both energy levels. With increasing pressure, the energy gap between the two levels increases, potentially inducing a transition to the low spin state with electrons only present in the lower energy level (e.g., Badro et al., 2003; Lin et al., 2007; Speziale et al., 2005; Tsuchiya et al., 2006; Wu & Wentzcovitch, 2014). At deep mantle temperatures, this transition is characterized by an increase in density of ~2–3% in Fp (Komabayashi et al., 2010; Mao et al., 2011). The iron spin transition in Bm is more complex due to two different crystallographic sites, an octahedral and a dodecahedral, and two different oxidation states of iron, Fe^{2+} and Fe^{3+} (see review by Lin et al., 2013, and references therein). Its detailed consequences on Bm thermodynamical and thermoelastic properties are still under debate (e.g., Glazyrin et al., 2014). Again, this iron spin transition may change physical properties such as density and elastic parameters (e.g., Badro et al., 2003; Lin et al., 2013; Wu & Wentzcovitch, 2014) and may further affect the dynamics of the Earth's mantle.

Previous models of thermal convection (e.g., Bower et al., 2009; Shahnas et al., 2011; Vilella et al., 2015) found that the presence of the iron spin transition increased mantle temperature and enhanced flow velocity. As the iron spin transition in Fp mainly occurs in the lower mantle, its dynamical effects on the long-term evolution of large thermochemical structures, such as LLSVPs, should be fully examined with thermochemical convection models. Huang et al. (2015) investigated the effects of the iron spin transition on the dynamics and topography of chemically distinct LLSVPs and suggested that LLSVPs are transient structures that last for 200 to 300 Myr, which is incompatible with a primordial origin of LLSVPs (i.e., early mantle differentiation). In this study, we follow the approach of Vilella et al. (2015) and extend it to thermochemical convection, to explore the effects of the iron spin transition on the long-term evolution of large primordial reservoirs in the lower mantle of the Earth.

2. Model Setup

2.1. Spin State Transition Model

To calculate the density of the lower mantle including the effect of the iron spin transition occurring in ferropericlase, we follow the model developed by Vilella et al. (2015), which is briefly presented below. The lower mantle is assumed to be pyrolitic with 18 vol% of ferropericlase, 75 vol% of Al-bearing Mg-bridgmanite, and 7 vol% of Ca-silicate bridgmanite, with 4.7 wt% of Al_2O_3 and 8 wt% of FeO, where 50% of iron is Fe^{2+} and 50% is Fe^{3+}. The average Fe^{2+} spin configuration in ferropericlase is calculated by minimizing the Helmholtz free energy following Sturhahn et al. (2005). We then combined the resulting average Fe^{2+} spin configuration with the Mie-Grüneisen-Debye equation of state (Jackson & Rigden, 1996) to obtain the density of the lower mantle as a function of pressure and temperature. It is important to note that the density change with iron spin transition obtained with this method is based on experimental data, and that these data implicitly account for the change in thermal expansion associated with this transition. Furthermore, the pressure and temperature dependencies of this density change are modeled using parameters (in particular, the bulk modulus, Debye temperature, and Grüneisen parameter at ambient conditions) deduced from experimental data and provide a good fit of these experimental results. Vilella et al. (2015) further assumed that the iron partitioning coefficient (K_D) between ferropericlase and bridgmanite changes with pressure following Irifune et al. (2010), with values around 0.8 and 0.4 at the top and bottom of the lower mantle, respectively. However, recent laboratory experiments (Piet et al., 2016; Prescher et al., 2014) found that K_D is constant with pressure. Following these latter experiments, we here assumed that K_D is constant throughout the mantle and equal to 0.5 (Piet et al., 2016). Figure 1a shows the relative density difference ($\Delta\rho = 100(\rho_{\mathrm{Spin}} - \rho_{\mathrm{Ref}})/\rho_{\mathrm{Spin}}$) between the model with spin state transition and the reference model (without spin state transition). As found by

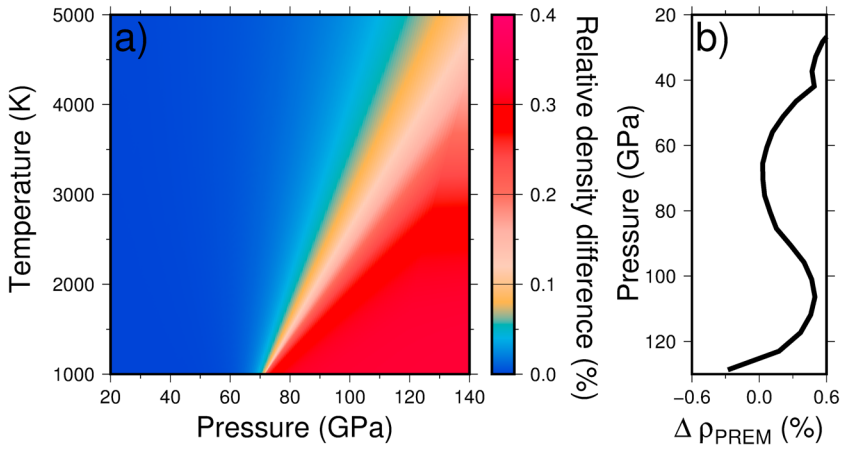

Figure 1. (a) Relative density difference (%) between the model with the iron spin transition and the reference model (without the iron spin transition), as a function of pressure and temperature. (b) Relative density difference (%) between the calculated density profile and PREM density.

theoretical and experimental studies, the spin state transition is sharp at low temperature and broad at high temperature. The amplitude of the density change is small, ~0.4%, and the calculated density profile agrees well with PREM density (Dziewonski & Anderson, 1981) (Figure 1b), and laboratory experiments conducted at high temperatures (Komabayashi et al., 2010; Mao et al., 2011).

2.2. Mantle Convection Model

We conducted numerical simulations of thermochemical convection using the code StagYY (Tackley, 2008) and modified it to include the density tables calculated following the method developed by Vilella et al., 2015 (section 2.1). StagYY solves the conservation equations of mass, momentum, energy, and composition for an anelastic compressible fluid with infinite Prandtl number. The numerical model is similar to that in Li et al. (2015), and only the key details are described here (see supporting information Text S1 for more details).

Our numerical experiments are performed in 2-D spherical annulus geometry with a grid of 129 radial nodes and 1,025 lateral nodes. Four million tracers are used to track the composition field, varying between 0 for ambient mantle material and 1 for primordial dense material. The density difference between primordial and ambient mantle materials is controlled by the buoyancy ratio (B) defined as

$$B = \frac{\Delta\rho_C}{\alpha_s \rho_s \Delta T_S} \tag{1}$$

where $\Delta\rho_C$ is the density difference between the dense (primordial) and regular (ambient) mantle materials. To explore the influence of B on the stability of primordial reservoirs, we varied this parameter between 0.18 and 0.26, corresponding to density differences between 72 kg/m^3 and 104 kg/m^3.

3. Results

In order to identify and quantify the effects of iron spin transition, we have conducted two series of numerical experiments, one with the iron spin transition and one without. To estimate the relative influence of iron spin transition compared to other controlling parameters, we further varied the buoyancy ratio, which has been found to be the main parameter controlling the stability of reservoirs of dense material (e.g., Deschamps & Tackley, 2009; Li et al., 2014a; McNamara & Zhong, 2004).

Figure 2a shows the snapshots at $t = 4.5$ Gyr of composition and temperature fields for reference cases ($B = 0.26$) with and without the iron spin transition. In the case without the iron spin transition, two antipodal large reservoirs of primordial dense material are observed at the bottom of the mantle. In the case with the iron spin transition, we again observe two antipodal reservoirs, but with slightly smaller sizes and sharper edges compared to the case without the iron spin transition. In addition, a third, much smaller reservoir is present. Snapshots of temperature fields indicate that plumes form at the top of primordial reservoirs and at their margins. In the case with the iron spin transition, convection is more vigorous. Plumes are therefore stronger (in particular, wider and hotter) and can even form outside the primordial reservoirs.

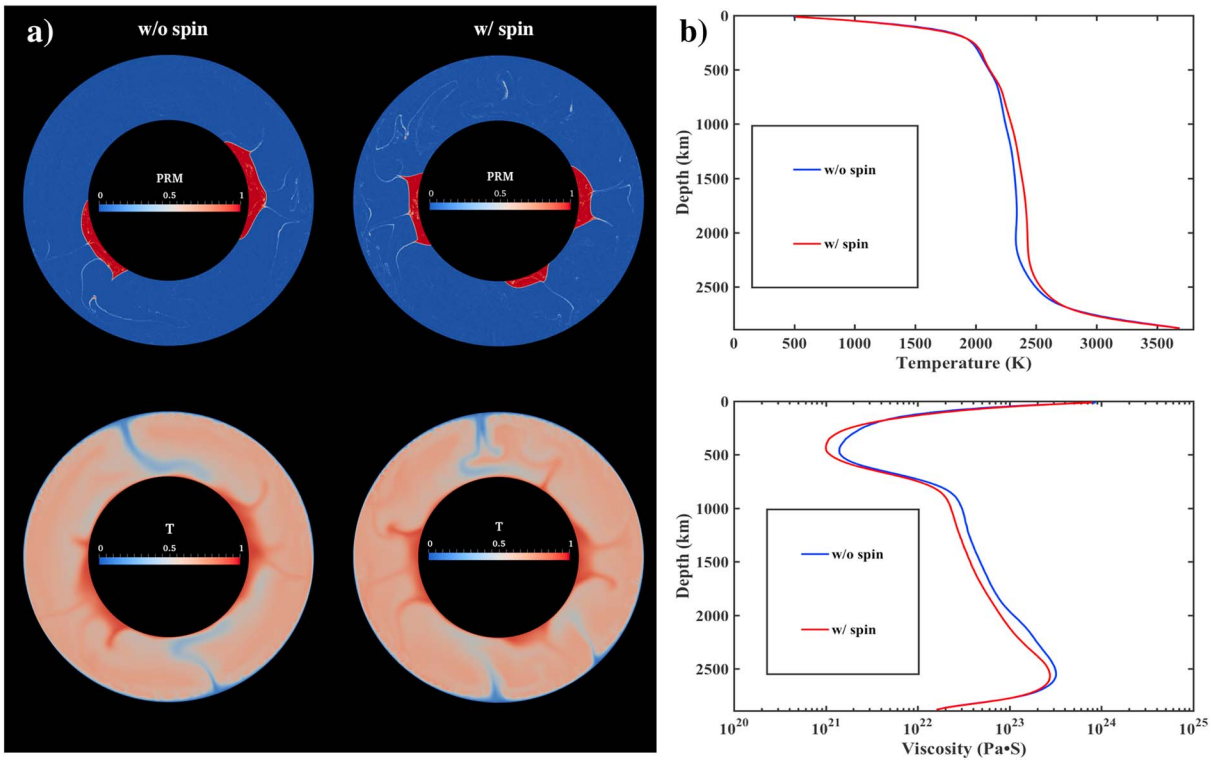

Figure 2. Reference cases ($B = 0.26$). (a) Snapshots of composition (top) and temperature (bottom) fields at $t = 4.5$ Gyr without (left) and with (right) the iron spin transition. (b) The 1-D profiles of horizontally averaged mantle temperature (top) and viscosity (bottom) without (blue curves) and with (red curves) the iron spin transition.

This makes the convective system more realistic when compared to Earth's mantle, where a few plumes (e.g., southeastern Australia and Yellowstone plumes) can be found outside LLSVPs (French & Romanowicz, 2015). The 1-D profiles of horizontally averaged temperature and viscosity for cases with and without the iron spin transition are very close to each other (Figure 2b). At depths ranging from the top of the lower mantle (700 km) down to 2,600 km (300 km above the CMB), the case with the iron spin transition has a slightly higher average temperature, in agreement with previous studies (e.g., Bower et al., 2009; Vilella et al., 2015). In the lowermost 300 km, horizontally averaged temperatures for cases with and without the iron spin transition are very similar, due to the fact that hot primordial reservoirs are slightly larger in the case without the iron spin transition, thus compensating the slightly higher temperature caused by the iron spin transition.

Figure 3a shows the snapshots of composition and temperature fields for small buoyancy ratio cases ($B = 0.18$) with and without the iron spin transition at $t = 4.5$ Gyr. Large reservoirs are now absent in both cases, and only one small, unstable, reservoir of primordial material can be found in the case without the iron spin transition. Again, 1-D profiles of horizontally averaged temperature and viscosity for cases with and without the iron spin transition are similar to each other. We note, however, that the average temperature in the lowermost mantle is slightly higher when the iron spin transition is not included, which can be explained by the larger amount of primordial material maintained in the lowermost mantle. Comparing cases with $B = 0.18$ and $B = 0.26$ suggests that the buoyancy ratio is the dominant parameter controlling the stability of the large primordial reservoirs of dense material, in agreement with previous studies (e.g., Deschamps & Tackley, 2009; Li et al., 2014a; McNamara & Zhong, 2004), while the iron spin transition only slightly promotes their destabilization.

In order to confirm these observations, we now try to quantify the stability of reservoirs of dense material. For this, we use different criteria. First, we plotted the evolution of the average altitude of primordial material (Figure 4), defined as

$$< H_c > = \frac{1}{V}\int_V C(r,\theta) r dV, \tag{2}$$

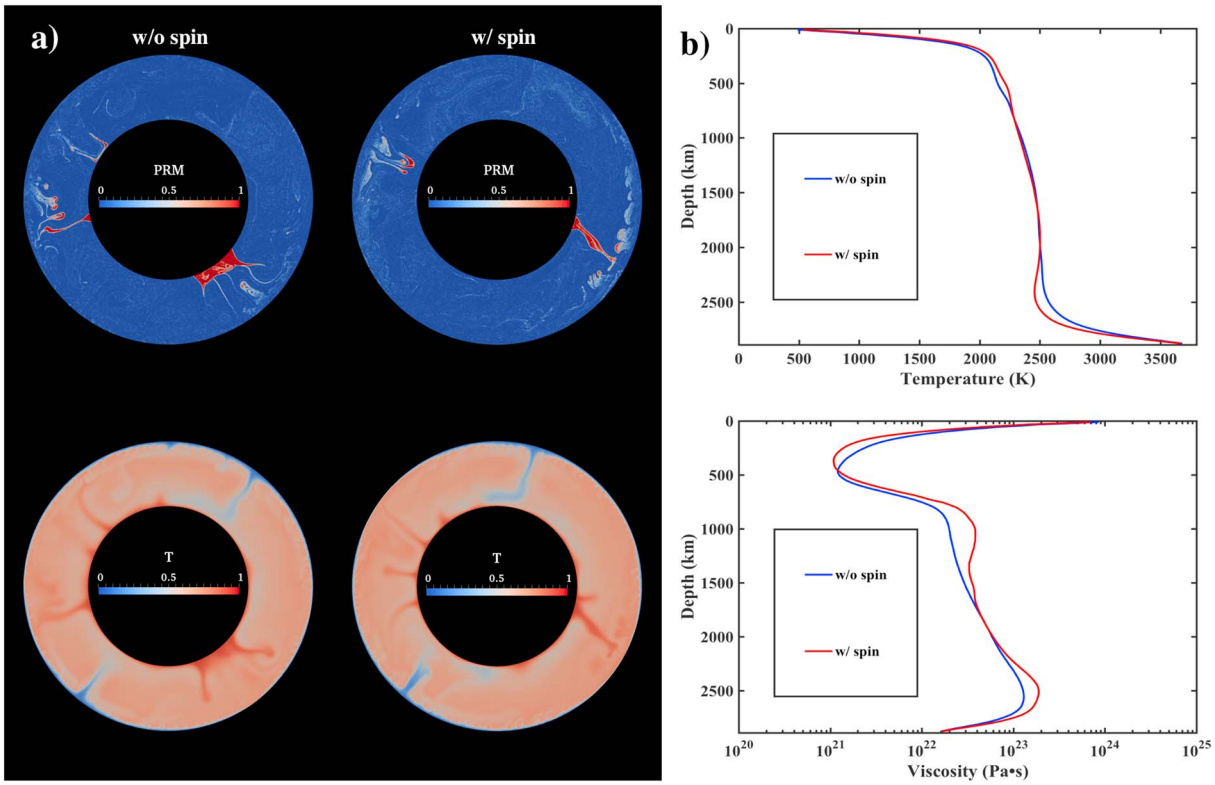

Figure 3. Small buoyancy ratio cases ($B = 0.18$). (a) Snapshots of composition (top) and temperature (bottom) fields at $t = 4.5$ Gyr without (left) and with (right) the iron spin transition. (b) The 1-D profiles of horizontally averaged mantle temperature (top) and viscosity (bottom) without (blue curves) and with (red curves) the iron spin transition.

which is an appropriate parameter to assess the mixing efficiency (e.g., Deschamps & Tackley, 2009; Li et al., 2014a). Small values of $< H_c >$, ~0.04, correspond to stable layering, while large values, ~0.6, indicate efficient mixing. We then calculated the fraction of primordial material remaining in the lowermost 300 km of the mantle, again as a function of time (Figure 5a), and the radial profile of the horizontally averaged fraction of primordial material at $t = 4.5$ Gyr (Figure 5b). These two parameters provide additional information on the distribution of primordial material throughout the system, and on the vertical extension of the reservoirs of dense material.

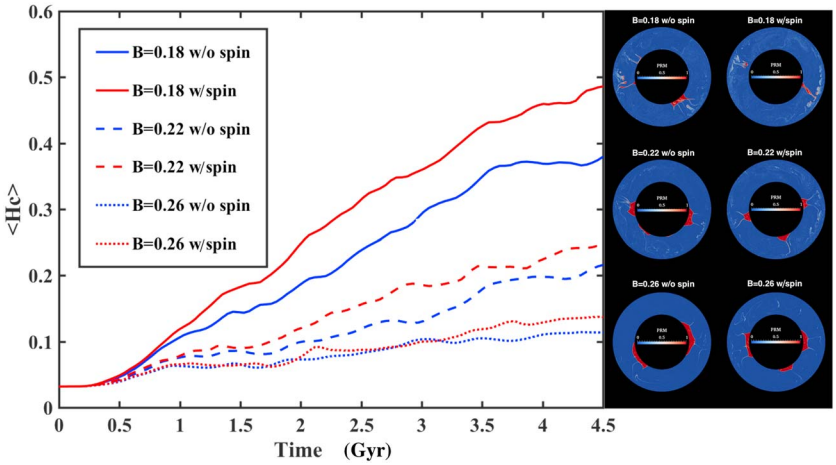

Figure 4. Average altitude of primordial materials ($< H_c >$, equation (2)) as a function of time for cases of $B = 0.18$, 0.22, 0.26 with (red curves) and without (blue curves) the iron spin transition. Right panel shows snapshots of composition fields at $t = 4.5$ Gyr for each case.

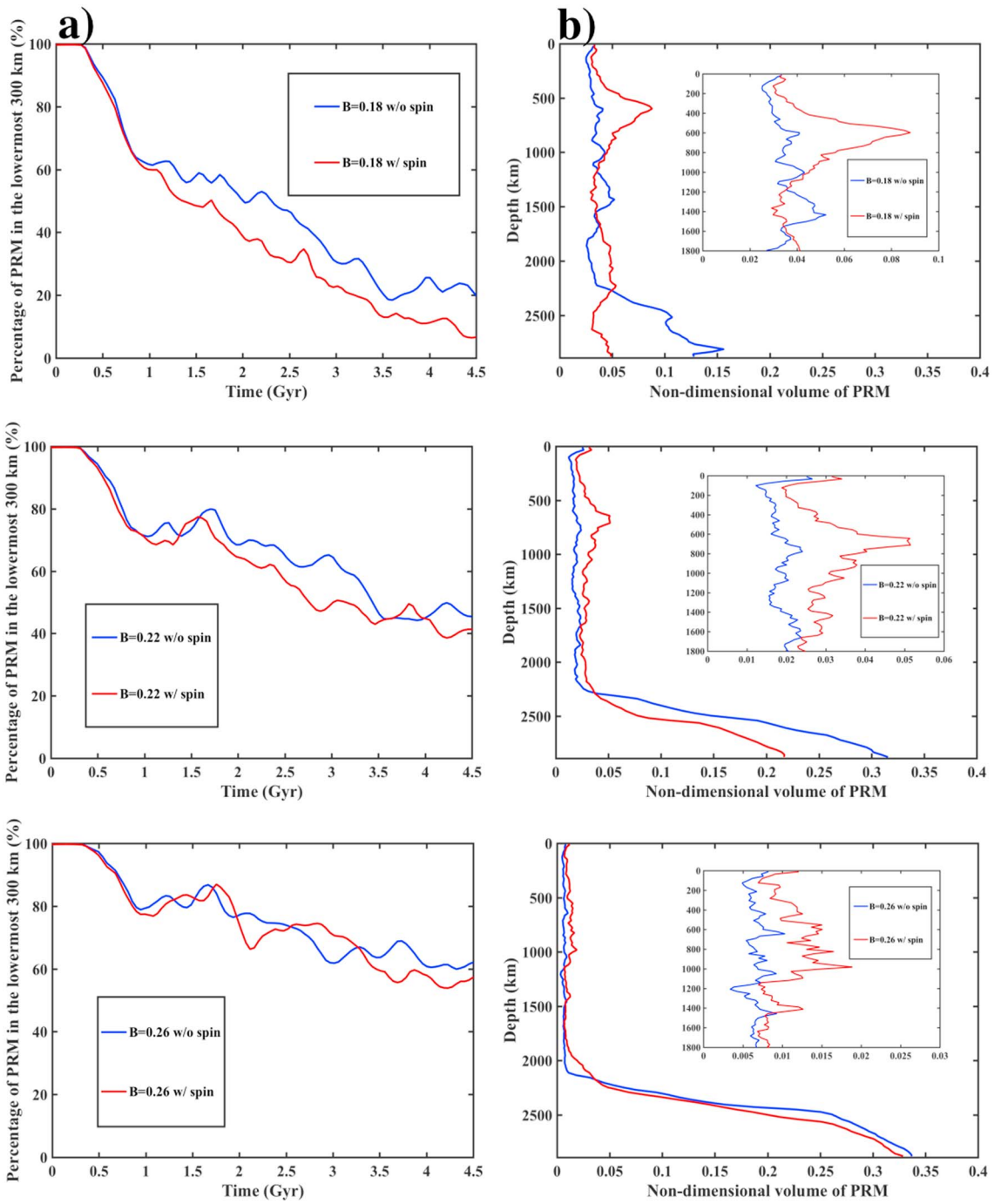

Figure 5. (a) Percentage of primordial material maintained in the lowermost 300 km of the mantle as a function of time and (b) 1-D profiles of distribution of primordial material in the mantle at $t = 4.5$ Gyr for $B = 0.18$ (top), 0.22 (middle), and 0.26 (bottom).

For $B = 0.18$, high values of $< H_c >$ (Figure 4) indicate that reservoirs of primordial material are unstable whether the iron spin transition is present or not. Instead, primordial materials are entrained by plumes into the upper mantle and are continuously mixed with ambient mantle material. For $B = 0.22$ and $B = 0.26$, in contrast, reservoirs of primordial material remain stable for cases with and without the iron spin transition, as shown by the moderate values of $< H_c >$. Interestingly, regardless of the values of the buoyancy ratio, $< H_c >$ is systematically higher when the iron spin transition is included. This confirms that the iron spin transition tends to produce less stable reservoirs. However, varying the buoyancy ratio impacts more importantly the time evolution of $< H_c >$. Furthermore, as the buoyancy ratio increases, the differences in $< H_c >$ between

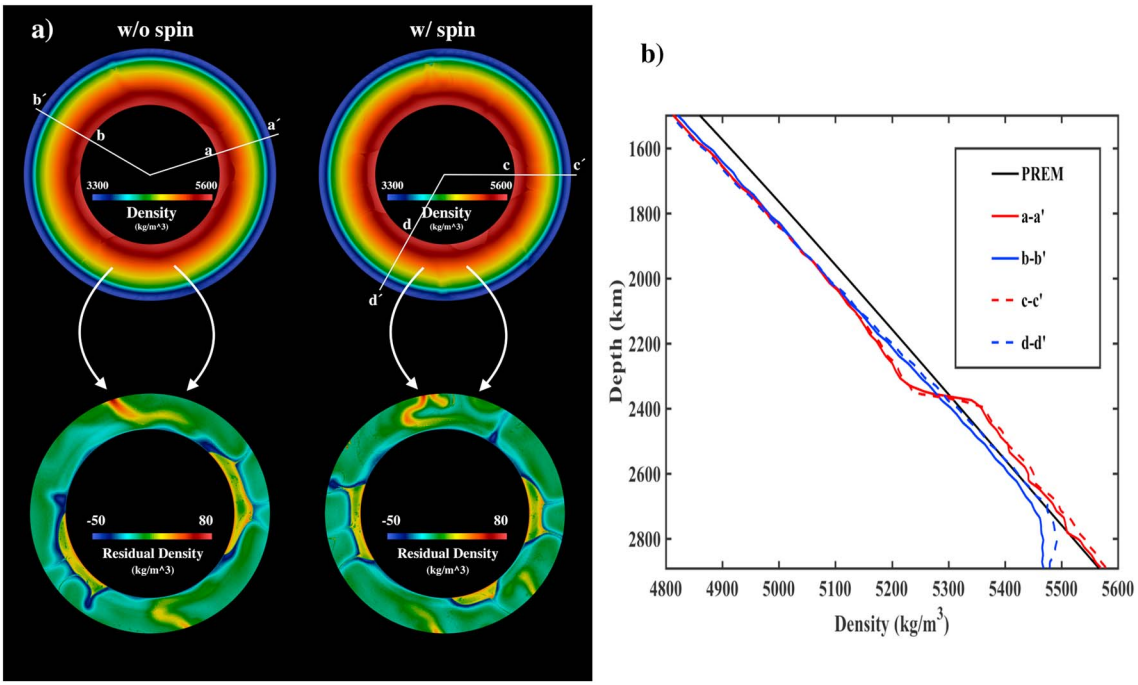

Figure 6. (a) Snapshots of density fields of the whole mantle (top) and residual density fields of the lower 1,400 km (bottom) at $t = 4.5$ Gyr for cases without (left) and with (right) the iron spin transition and for buoyancy ratio $B = 0.26$, (b) radial profiles of density drawn along radii a-a′, b-b′, c-c′, and d-d′ in plot (a), and PREM. Profiles a-a′ and c-c′ sample large primordial reservoirs and profiles b-b′ and d-d′ sample regular mantle. Only the lower 1,400 km are shown.

cases with and without the iron spin transition decrease, suggesting that the relative influence of iron spin transition decreases as the buoyancy ratio increases.

Figure 5b shows radial profiles of primordial material at 4.5 Gyr for all six experiments. In the cases with $B = 0.26$, radial distributions of primordial material are similar, and only small amount of primordial material can be observed in the upper mantle due to the phase change at 660 km, which prevents most of the dense primordial material from being entrained to the upper mantle (e.g., Deschamps & Tackley, 2009; Li et al., 2014a). Between 660-km depth and the top of large primordial reservoirs, more primordial material is present in the case accounting for the iron spin transition than in the case without this transition, which again indicates that the large primordial reservoirs are slightly less stable. Note that although the amount of primordial material is larger in the cases including the iron spin transition, the total amount of primordial material in these regions is very small, indicating that the large scale stability is not substantially altered by the iron spin transition. Figure 5a shows the fraction of primordial material in the lowermost 300 km as a function of time for all six experiments. As one would expect, the amount of primordial material in the lowermost mantle increases as the buoyancy ratio increases. For $B = 0.18$, the amount of primordial material in the lowermost 300 km sharply decreases with time. By the end of the experiment, it reaches 20% for the case without the iron spin transition, and only ~10% in the case with the iron spin transition. Again, for this value of B, the presence of the iron spin transition further decreases the stability of the reservoirs of dense material. For $B = 0.22$, the difference between cases with and without the iron spin transition is much smaller, and most importantly, more than 40% of the primordial material remains in the lowermost 300 km at the end of the calculations in both cases. For $B = 0.26$, the evolution of the amount of primordial material in the lowermost mantle is nearly independent of the presence of the iron spin transition and slowly decreases down to 60% at the end of the experiments. Together with the evolution of $< H_C >$, this shows that large primordial reservoirs can be maintained in the lowermost 300 km whether the iron spin transition is present or not. For $B = 0.26$, the fraction of the core-mantle boundary (CMB) covered by primordial reservoirs is 33% in the case with the iron spin transition, which is nearly the same as in the case without the iron spin transition (34%; Figure 5b). Note that these values are in reasonable agreement with the estimated surface covered by LLSVPs (e.g., Garnero et al., 2016). The fraction of the CMB region covered by primordial reservoirs decreases with decreasing buoyancy ratio. Interestingly, at $B = 0.22$, the dense material covers a much smaller area if the iron spin transition is present (around 22%) than if it is not (around 31%). When the buoyancy ratio is reduced to 0.18, although neither case

can maintain large primordial reservoirs, the fraction of the CMB covered by primordial material in the case with the iron spin transition is, again, significantly smaller than in the case without the iron spin transition. Therefore, if primordial reservoirs are not dense enough compared to the surrounding mantle, their stability may be strongly affected by the iron spin transition, in which case they become transient structures.

Overall, our experiments indicate that the density change triggered by the iron spin transition plays a minor role compared to the effect of the buoyancy ratio, and that its influence is more important in cases with a small buoyancy ratio (<0.2) than in cases with a higher buoyancy ratio. This may provide useful hints to infer the nature of LLSVPs, as discussed in the next section.

4. Discussion and Conclusions

In this study, we investigated the effects of the iron spin transition on the stability and structure of large primordial reservoirs in the Earth's lower mantle. Similarly to previous studies (Bower et al., 2009; Shahnas et al., 2011; Vilella et al., 2015), we found that the iron spin transition enhances the convective vigor and increases mantle temperatures except in the lowermost several hundred kilometers, where the hot primordial reservoirs are larger in the cases without the iron spin transition, leading to higher average temperatures. Because large primordial reservoirs are hotter than ambient mantle material, the density increase due to the iron spin transition is larger in cold regions (see Figure 1a), thus reducing the density contrast between primordial and ambient mantle materials. The effect of iron spin transition is therefore similar to lowering the buoyancy ratio, i.e., a decrease in stability of the reservoirs of dense material.

In order to further quantify the relative importance of buoyancy ratio and iron spin transition on the stability of large primordial reservoirs, we plotted the density fields obtained for $B = 0.26$ (Figure 6). These distributions do not show significant differences depending on the presence or absence of the iron spin transition, in agreement with previous studies suggesting that the broad and smooth iron spin transition might not produce obvious signatures in the radial velocity or density profile (Cammarano et al., 2010; Wu & Wentzcovitch, 2014; Wu et al., 2013). We then extracted the residual density in the lower 1,400 km. Interestingly, we observed that when the iron spin transition is not included, the lighter regions (blue regions in Figure 6a) surrounding the large primordial reservoirs are larger than when the iron spin transition is included. This favors the spreading of large primordial reservoirs along the CMB and the formation of smooth edges. Meanwhile, in the case with the iron spin transition, smaller and lighter regions lead to reservoirs with sharper edges. Figure 6b compares radial density profiles drawn either inside or outside the large primordial reservoirs (white lines on density maps), for cases with and without the iron spin transition. At depths shallower than 2,000 km, radial density profiles are very similar in all cases. Differences appear in the lowermost mantle. First, the profiles sampling the reservoirs of dense material (red curves) are denser than the profiles sampling the regular mantle (blue curves) by about 100 kg/m^3, as one would expect for $B = 0.26$. Second, for similar locations, the profiles obtained with iron spin transition are slightly denser than those obtained without. Importantly, this difference is only about ~10 kg/m^3, that is, 1 order of magnitude smaller than the difference between dense material and regular mantle. Again, this demonstrates that the buoyancy ratio is the dominant parameter controlling the properties of the large primordial reservoirs. One may point out that the increase in density due to the iron spin transition is larger outside the primordial reservoir. This is related to thermal effects (Figure 1), which tend to decrease the density contrast between primordial and ambient materials. This small decrease in density contrast reduces, in principle, the stability of the primordial reservoirs. Practically, however, it is again too small, compared to the density contrast between dense and regular material, to have significant effects on the stability of the primordial reservoirs.

While the iron spin transition in the lower mantle does not alter the long-term stability of large primordial reservoirs, it triggers other effects that are worth mentioning. As pointed out by previous studies (Bower et al., 2009; Vilella et al., 2015), enhanced convection allows cold downwellings to reach and spread along the CMB more easily in cases including the iron spin transition. These cold downwellings push aside the primordial reservoirs, and promote the development of plumes from the edges. They further help to sharpen the edges of primordial reservoirs, as observed in seismological studies (e.g., Ni et al., 2002). These effects are similar to those caused by postperovskite, which also causes a density increase due to the phase change (e.g., Li et al., 2014b; Nakagawa & Tackley, 2005).

Our results contrast with the previous work of Huang et al. (2015), which suggests that iron spin transition induces unstable piles. This disagreement may be related to differences in the modeling of the iron spin

transition, which we now briefly discuss. A first possible source of discrepancy lies in the data used to model the density jump induced by the iron spin transition. Huang et al., 2015's simulations mainly used data from first principle calculations of Wu et al. (2009). Based on these data, and for a mantle composed of 20% ferropericlase, they assume a density jump up to ∼1%. Following this estimate, the density increase induced by iron spin transition in ferropericlase alone would be ∼5%. By contrast, experimental results conducting at high pressure and temperature suggest a density difference of only 1.8%–2.4% (see Lin et al., 2013, for a review), the exact value depending on the iron content in ferropericlase. In this study, we followed the study by Vilella et al. (2015) and assumed a density difference of ∼0.4% in total density induced by iron spin transition for a mantle composed of 18% ferropericlase, which is equivalent to a density increase of ∼2.2% in ferropericlase, thus in good agreement with the experimental results (e.g., Lin et al., 2013; Mao et al., 2011). Since the iron spin transition favors lower temperature condition (Figure 1a), the increasing density change by the iron spin transition decreases the density contrast between the hot, dense LLSVP and the ambient mantle. The different data used in our study and Huang et al. (2015) may partly explain the different patterns of LLSVPs' stability observed in these two studies. In addition, the numerical treatment of the density changes may introduce further discrepancies. To model these changes, Huang et al. (2015) uses the extended Boussinesq approximation, while in our study they are directly calculated from density tables based on experimental data, which implicitly include the effects of the iron spin transition on thermal expansion and bulk modulus, and thermodynamical modeling. Besides the differences in density models, differences in the parameters of the simulations may partly explain the disagreement between our results and those of Huang et al. (2015). In particular, Huang et al. (2015) used a smaller thermal viscosity contrast than in our simulations. This leads to a more vigorous convection and increases the entrainment of dense material by increasing the viscous coupling. This, in turn, promotes the transient nature of the reservoirs of dense material, independently of the presence of the iron spin transition.

Overall, by considering a low thermal viscosity contrast and, most importantly, low density contrast between the ambient material and dense material. Huang et al. (2015) simulations favor a transient nature for reservoirs of dense material. In contrast, our simulations indicate that the stability of piles are mainly controlled by the buoyancy ratio, as pointed out in previous studies (e.g., Deschamps & Tackley, 2009; Li et al., 2014a; McNamara & Zhong, 2004). In particular, for buoyancy ratios corresponding to chemical density contrasts of ∼100 kg/m^3 and larger, as it is expected for the LLSVPs (e.g., Trampert et al., 2004), the alteration caused by the iron spin transition is not strong enough to modify the long-term stability of large primordial reservoirs. For smaller buoyancy ratios, corresponding to density contrast ∼70 kg/m^3 or less, reservoirs are unstable independently of the presence of the iron spin transition.

An important approximation of our current models is that the iron spin transition was assumed to have the same effects on the primordial material and the ambient mantle material. However, if LLSVPs are enriched in iron (e.g., Deschamps et al., 2012; Trampert et al., 2004), the effect of the iron spin transition should be stronger in LLSVPs. This may not substantially modify the stability of LLSVPs since, as shown by our simulations, the buoyancy ratio remains the controlling parameter. It could, however, strongly impact the interpretation of seismic observations in term of iron. Accounting for different compositions for the primordial reservoirs is therefore needed to improve our modeling. This approach may in turn provide additional constraints on the possible compositions of LLSVPs. Furthermore, the thermal conductivity of LLSVPs may be strongly affected since this property is impacted by the iron content (Hsieh et al., 2017) and to a lesser extent by the iron spin transition (Hsieh et al., 2018). This need to be investigated in future work.

Acknowledgments
We are grateful to the Editors, Jeroen Ritsema and Mingming Li, and the reviewers, Wei Leng and Ctirad Matyska, for the constructive reviews on an earlier version of this manuscript and Zhigang Zhang for helpful discussion. This research was supported by National Natural Science Foundation of China (NSFC) grants 41704100, 41625016, 41374067, and 41404073, Ministry of Science and Technology of Taiwan (MOST) grant 105-2116-M-001-017, and Academia Sinica (Taipei, Taiwan) grant AS-102-CDA-M02. Y. L. was supported by Pioneer Hundred Talents Program, Chinese Academy of Sciences. The calculations were performed on Tianhe-1(A) at National Supercomputer Center in Tianjin. We note that there are no data sharing issues since all of the numerical information is provided in the figures produced by solving the equations in the paper and supporting information.

References

Badro, J., Fiquet, G., Guyot, F., Rueff, J.-P., Struzhkin, V. V., Vankó, G., & Monaco, G. (2003). Iron partitioning in Earth's mantle: Toward a deep lower mantle discontinuity. *Science*, *300*(5620), 789–791.

Badro, J., Rueff, J.-P., Vankó, G., Monaco, G., Fiquet, G., & Guyot, F. (2004). Electronic transitions in perovskite: Possible nonconvecting layers in the lower mantle. *Science*, *305*(5682), 383–386.

Bower, D. J., Gurnis, M., Jackson, J. M., & Sturhahn, W. (2009). Enhanced convection and fast plumes in the lower mantle induced by the spin transition in ferropericlase. *Geophysical Research Letters*, *36*, L10306. https://doi.org/10.1029/2009GL037706

Boyet, M., & Carlson, R. W. (2006). A new geochemical model for the Earth's mantle inferred from ^{146}Sm–^{142}Nd systematics. *Earth and Planetary Science Letters*, *250*(1-2), 254–268. https://doi.org/10. 1016/j.epsl.2006.07.046

Cammarano, F., Marquardt, H., Speziale, S., & Tackley, P. J. (2010). Role of iron-spin transition in ferropericlase on seismic interpretation: A broad thermochemical transition in the mid mantle? *Geophysical Research Letters*, *37*, L03308. https://doi.org/10.1029/2009GL041583

Cohen, R. E., Mazin, I., & Isaak, D. G. (1997). Magnetic collapse in transition metal oxides at high pressure: Implications for the Earth. *Science*, *275*(5300), 654–657.

Deschamps, F., Cobden, L., & Tackley, P. J. (2012). The primitive nature of large low shear-wave velocity provinces. *Earth and Planetary Science Letters*, *349-350*, 198–208. https://doi.org/10.1016/j.epsl.2012.07.012

Deschamps, F., & Tackley, P. J. (2009). Searching for models of thermo-chemical convection that explain probabilistic tomography. II: Influence of physical and compositional parameters. *Physics of the Earth and Planetary Interiors*, *176*(1-2), 1–18. https://doi.org/10.1016/j.pepi.2009.03.012

Dziewonski, A. M., & Anderson, D. L. (1981). Preliminary reference Earth model. *Physics of the Earth and Planetary interiors*, *25*(4), 297–356.

Farley, K., Natland, J., & Craig, H. (1992). Binary mixing of enriched and undegassed (primitive?) mantle components (He, Sr, Nd, Pb) in Samoan lavas. *Earth and Planetary Science Letters*, *111*(1), 183–199. https://doi.org/10.1016/0012-821X(92)90178-X

French, S. W., & Romanowicz, B. (2015). Broad plumes rooted at the base of Earth's mantle beneath major hotspots. *Nature*, *525*, 95–99.

Fyfe, W. (1960). The possibility of d-electron coupling in olivine at high pressures. *Geochimica et Cosmochimica Acta*, *19*(2), 141–143. https://doi.org/10.1016/0016-7037(60)90046-6

Garnero, E. J., McNamara, A. K., & Shim, S.-H. (2016). Continent-sized anomalous zones with low seismic velocity at the base of Earth's mantle. *Nature Geoscience*, *9*, 481–489.

Glazyrin, K., Ballaran, T. B., Frost, D., McCammon, C., Kantor, A., Merlini, M., et al. (2014). Magnesium silicate perovskite and effect of iron oxidation state on its bulk sound velocity at the conditions of the lower mantle. *Earth and Planetary Science Letters*, *393*, 182–186.

He, Y., & Wen, L. (2012). Geographic boundary of the Pacific anomaly and its geometry and transitional structure in the north. *Journal of Geophysical Research*, *117*, B09308. https://doi.org/10.1029/2012JB009436

Hofmann, A. (1997). Mantle geochemistry: The message from oceanic volcanism. *Nature*, *385*(6613), 219–229. https://doi.org/10.1038/385219a0

Hsieh, W.-P., Deschamps, F., Okuchi, T., & Lin, J.-F. (2017). Reduced lattice thermal conductivity of Fe-bearing bridgmanite in the Earth's deep mantle. *Journal of Geophysical Research: Solid Earth*, *122*, 4900–4917. https://doi.org/10.1002/2017JB014339

Hsieh, W.-P., Deschamps, F., Okuchi, T., & Lin, J.-F. (2018). Effects of iron on the lattice thermal conductivity of Earth's deep mantle and implications for mantle dynamics. *Proceedings of the National Academy of Sciences of the United States of America*, *115*, 4099–4104. https://doi.org/10.1073/pnas.1718557115

Huang, C., Leng, W., & Wu, Z. (2015). Iron-spin transition controls structure and stability of LLSVPs in the lower mantle. *Earth and Planetary Science Letters*, *423*, 173–181. https://doi.org/10.1016/j.epsl.2015.05.006

Irifune, T., Shinmei, T., McCammon, C. A., Miyajima, N., Rubie, D. C., & Frost, D. J. (2010). Iron partitioning and density changes of pyrolite in Earth's lower mantle. *Science*, *327*(5962), 193–195.

Ishii, M., & Tromp, J. (1999). Normal-mode and free-air gravity constraints on lateral variations in velocity and density of Earth's mantle. *Science*, *285*(5431), 1231–1236. https://doi.org/10.1126/science.285.5431.1231

Jackson, I., & Rigden, S. M. (1996). Analysis of PVT data: Constraints on the thermoelastic properties of high-pressure minerals. *Physics of the Earth and Planetary Interiors*, *96*(2-3), 85–112.

Jackson, J. M., Sturhahn, W., Shen, G., Zhao, J., Hu, M. Y., Errandonea, D., et al. (2005). A synchrotron Mössbauer spectroscopy study of (Mg, Fe) SiO_3 perovskite up to 120 GPa. *American Mineralogist*, *90*(1), 199–205.

Koelemeijer, P., Deuss, A., & Ritsema, J. (2017). Density structure of Earth's lowermost mantle from Stoneley mode splitting observations. *Nature Communications*, *8*, 15241.

Komabayashi, T., Hirose, K., Nagaya, Y., Sugimura, E., & Ohishi, Y. (2010). High-temperature compression of ferropericlase and the effect of temperature on iron spin transition. *Earth and Planetary Science Letters*, *297*(3), 691–699.

Kuo, C., & Romanowicz, B. (2002). On the resolution of density anomalies in the Earth's mantle using spectral fitting of normal-mode data. *Geophysical Journal International*, *150*, 162–179.

Labrosse, S., Hernlund, J., & Coltice, N. (2007). A crystallizing dense magma ocean at the base of the Earth's mantle. *Nature*, *450*(7171), 866–869.

Lau, H. C. P., Mitrovica, J. X., Davis, J. L., Tromp, J., Yang, H.-Y., & Al-Attar, D. (2017). Tidal tomography constraints Earth's deep mantle buoyancy. *Nature*, *551*, 321–326.

Li, Y., Deschamps, F., & Tackley, P. J. (2014a). The stability and structure of primordial reservoirs in the lower mantle: Insights from models of thermochemical convection in three-dimensional spherical geometry. *Geophysical Journal International*, *199*(2), 914–930. https://doi.org/10.1093/gji/ggu295

Li, Y., Deschamps, F., & Tackley, P. J. (2014b). Effects of low-viscosity post-perovskite on the stability and structure of primordial reservoirs in the lower mantle. *Geophysical Research Letters*, *41*, 7089–7097. https://doi.org/10.1002/2014GL061362

Li, Y., Deschamps, F., & Tackley, P. J. (2015). Effects of the post-perovskite phase transition properties on the stability and structure of primordial reservoirs in the lower mantle of the Earth. *Earth and Planetary Science Letters*, *432*, 1–12. https://doi.org/10.1016/j.epsl.2015.09.040

Lin, J.-F., Speziale, S., Mao, Z., & Marquardt, H. (2013). Effects of the electronic spin transitions of iron in lower mantle minerals: Implications for deep mantle geophysics and geochemistry. *Reviews of Geophysics*, *51*, 244–275. https://doi.org/10.1002/rog.20010

Lin, J.-F., Vankó, G., Jacobsen, S. D., Iota, V., Struzhkin, V. V., Prakapenka, V. B., et al. (2007). Spin transition zone in Earth's lower mantle. *Science*, *317*(5845), 1740–1743.

Lupton, J., & Craig, H. (1975). Excess ^{3}He in oceanic basalts: Evidence for terrestrial primordial helium. *Earth and Planetary Science Letters*, *26*(2), 133–139. https://doi.org/10.1016/0012-821X(75)90080-1

Mao, Z., Lin, J.-F., Liu, J., & Prakapenka, V. B. (2011). Thermal equation of state of lower-mantle ferropericlase across the spin crossover. *Geophysical Research Letters*, *38*, L23308. https://doi.org/10.1029/2011GL049915

Masters, G., Laske, G., Bolton, H., & Dziewonski, A. (2000). The relative behavior of shear velocity, bulk sound speed, and compressional velocity in the mantle: Implications for chemical and thermal structure. In S. Karato, et al. (Eds.), *Earth's deep interior: Mineral physics and tomography from the atomic to the global scale* (Vol. 117, pp. 63–87). Washington, DC: American Geophysical Union.

McNamara, A. K., & Zhong, S. (2004). Thermochemical structures within a spherical mantle: Superplumes or piles? *Journal of Geophysical Research*, *109*, B07402. https://doi.org/10.1029/2003JB002847

Mosca, I., Cobden, L., Deuss, A., Ritsema, J., & Trampert, J. (2012). Seismic and mineralogical structures of the lower mantle from probabilistic tomography. *Journal of Geophysical Research*, *117*, B06304. https://doi.org/10.1029/2011JB008851

Nakagawa, T., & Tackley, P. J. (2005). The interaction between the post-perovskite phase change and a thermo-chemical boundary layer near the core-mantle boundary. *Earth and Planetary Science Letters*, *238*(1), 204–216.

Ni, S., Tan, E., Gurnis, M., & Helmberger, D. (2002). Sharp sides to the African superplume. *Science*, *296*(5574), 1850–1852. https://doi.org/10.1126/science.1070698

Piet, H., Badro, J., Nabiei, F., Dennenwaldt, T., Shim, S.-H., Cantoni, M., et al. (2016). Spin and valence dependence of iron partitioning in Earth's deep mantle. *Proceedings of the National Academy of Sciences of the United States of America*, *113*(40), 11,127–11,130. https://doi.org/10.1073/pnas.1605290113

Prescher, C., Langenhorst, F., Dubrovinsky, L. S., Prakapenka, V. B., & Miyajima, N. (2014). The effect of Fe spin crossovers on its partitioning behavior and oxidation state in a pyrolitic Earth's lower mantle system. *Earth and Planetary Science Letters*, *399*, 86–91.

Shahnas, M., Peltier, W., Wu, Z., & Wentzcovitch, R. (2011). The high-pressure electronic spin transition in iron: Potential impacts upon mantle mixing. *Journal of Geophysical Research*, *116*, B08205. https://doi.org/10.1029/2010JB007965

Solomatov, V. S., & Stevenson, D. J. (1993). Suspension in convective layers and style of differentiation of a terrestrial magma ocean. *Journal of Geophysical Research*, *98*(E3), 5375–5390. https://doi.org/10.1029/92JE02948

Speziale, S., Milner, A., Lee, V., Clark, S., Pasternak, M., & Jeanloz, R. (2005). Iron spin transition in Earth's mantle. *Proceedings of the National Academy of Sciences of the United States of America*, *102*(50), 17,918–17,922.

Sturhahn, W., Jackson, J. M., & Lin, J.-F. (2005). The spin state of iron in minerals of Earth's lower mantle. *Geophysical Research Letters*, *32*, L12307. https://doi.org/10.1029/2005GL022802

Tackley, P. J. (2008). Modelling compressible mantle convection with large viscosity contrasts in a three-dimensional spherical shell using the yin-yang grid. *Physics of the Earth and Planetary Interiors*, *171*(1-4), 7–18. https://doi.org/10.1016/j.pepi.2008.08.005

Torsvik, T. H., van der Voo, R., Doubrovine, P. V., Burke, K., Steinberger, B., Ashwal, L. D., et al. (2014). Deep mantle structure as a reference frame for movements in and on the Earth. *Proceedings of the National Academy of Sciences of the United States of America*, *111*, 8735–8740. https://doi.org/10.1073/pnas.1318135111

Trampert, J., Deschamps, F., Resovsky, J., & Yuen, D. (2004). Probabilistic tomography maps chemical heterogeneities throughout the lower mantle. *Science*, *306*(5697), 853–856. https://doi.org/10.1126/science.1101996

Tsuchiya, T., Wentzcovitch, R. M., da Silva, C. R., & de Gironcoli, S. (2006). Spin transition in magnesiowüstite in Earth's lower mantle. *Physical Review Letters*, *96*(19), 198501.

Vilella, K., Shim, S.-H., Farnetani, C. G., & Badro, J. (2015). Spin state transition and partitioning of iron: Effects on mantle dynamics. *Earth and Planetary Science Letters*, *417*, 57–66.

Wang, Y., & Wen, L. (2007). Geometry and P and S velocity structure of the African anomaly. *Journal of Geophysical Research*, *112*, B05313. https://doi.org/10.1029/2006JB004483

Wu, Z., Justo, J. F., Da Silva, C. R. S., De Gironcoli, S., & Wentzcovitch, R. M. (2009). Anomalous thermodynamic properties in ferropericalse throughout its spin crossover. *Physical Review B*, *80*, 014409.

Wu, Z., Justo, J. F., & Wentzcovitch, R. M. (2013). Elastic anomalies in a spin-crossover system: Ferropericlase at lower mantle conditions. *Physical Review Letters*, *110*, 228501. https://doi.org/10.1103/PhysRevLett.110.228501

Wu, Z., & Wentzcovitch, R. M. (2014). Spin crossover in ferropericlase and velocity heterogeneities in the lower mantle. *Proceedings of the National Academy of Sciences of the United States of America*, *111*(29), 10,468–10,472.